# Morpholino-based peptide oligomers: synthesis and DNA binding properties

Alessandro Contini[1], Emanuela Erba[1], Valeria Bondavalli[1], Alberto Barbiroli[2], Maria Luisa Gelmi[1] and Alessandra Romanelli[1]*

[1] Dipartimento di Scienze Farmaceutiche,  Università degli Studi di Milano, Milano- Italy


[2] DeFENS -  Dipartimento di Scienze per gli Alimenti, la Nutrizione e l'Ambiente, Università degli Studi di Milano, Milano- Italy

*Corresponding author

e-mail: alessandra.romanelli @unimi.it

**Highlights**

Morpholino-peptide based oligomers show a preferred secondary structure

Morpholino-glycine based oligomers form complexes with DNA in a 2: 1 molar ratio

The complex between morpholino-glycine oligomers and DNA is stabilized by hydrophobic contacts between nucleobases and H-bonds beween the morpholino-peptide backbone.

**Abstract**

The chemical structure of oligonucleotide analogues dictates the conformation of oligonucleotide analogue oligomers , their ability to hybridize complementary DNA and RNA, their stability to degradation and their pharmacokinetic properties. In a study aimed at investigating new analogues featuring of a neutral backbone, we explored the ability of oligomers containing a morpholino-peptide backbone to bind oligonucleotides. Circular Dichroism studies revealed the ability of our oligomers to interact with DNA, molecular modelling studies revealed the interaction responsible for complex stabilization.

**Introduction**

Oligonucleotide analogues have been widely explored due to their potential application as drugs targeting nucleic acids and proteins. Modifications to the sugar moiety, to the nucleobase or to the phosphodiester backbone result in analogues with greater stability toward nucleases, increased affinity and specificity toward their target and finally improved pharmacokinetics properties as compared to natural oligonucleotides.[1]

Analogues such as morpholinos (PMO) and peptide nucleic acids (PNA) lack of charge on the backbone; this turns in a decreased electrostatic repulsion with the complementary DNA and RNA strand and therefore in a very high affinity and specificity of binding[2],[3]. In addition, PNA and PMO show high stability toward nucleases and are therefore ideal candidates as drugs. Today oligonucleotide analogues are employed in the clinic; notable examples are represented by the 30-mer PMO eterlipsen, an antisense for the treatment of the Duchenne muscular dystrophy, and by nusinersen, a 2'-O-MOE PS single stranded oligonucleotide modified at the backbone and at the sugar respectively by phosphorothioates and 2'-O-methoxyethyls, this last approved by FDA in 2016 for the cure spinal muscular atrophy. Other examples can be found in the literature[4].

The ability of oligonucleotides to self-assemble following Watson-Crick rules to give complex structures as cages allowed their exploitation as tools for the intracellular delivery of drugs[5],[6]. Very recently, the ability of nucleotides to self-assemble affording luminescent structures has been reported[7],[8]. Interesting studies have been reported on molecules containing a peptide backbone, such as PNA and nucleopeptides, to produce new materials [9],[10]. Li et al demonstrated that the conjugation of a nucleoside to phenyalanine and to a sugar moiety produces hydrogels able to bind  nucleic acids[11]. Nucleopeptides composed of complementary nucleobases connected at the N- terminus of peptides derived from the dimerization domains of larger proteins form hydrogels in which the molecules are organized in helices. From the combination of non-covalent interactions between peptides and nucleobases it is in principle possible to generate new structures. In this context, studies on the conformation of new nucleotide analogues and on their ability to bind oligonucleotide are of interest and will help in understanding critical requirements for hybridization *vs* aggregation.

We recently observed that short three- or hexa-peptides containing morpholino β-amino acids showed a conformational preference for type II polyproline helices or α-helix, depending on the

substitution pattern on the ring, due to the ability of the morpholino amino acid to form a H-bond between its oxygen and the NH of amino acid i+1 stabilizing a $\gamma$-turn conformation of the tripeptide construct.[12]

In this work we explored the potential of new nucleopeptide oligomers (Figure 1) to form complexes with DNA complementary strands. As compared to PMO, the new analogues lack of the phosphoramidate backbone. These oligomers are composed by a morpholino unit, functionalized with the nucleobase, alternated with a natural amino acid. The presence of the morpholino ring could impose conformational restrictions to the backbone, thus affecting hybridization properties of our oligomers.

The choice of the natural $\alpha$-amino acid to be inserted in the backbone, both for its side chain and chirality, can further increases the number of possible analogues that may be explored. In this work both glycine and alanine were selected, the former to increase the backbone flexibility, the latter for its ability to stabilize helix constructs[13].

Aim of this work is to: 1) develop a synthetic protocol for the solid-phase synthesis of oligomers containing alternated morpholino nucleosides and amino acids and 2) test the ability of the new oligomers to hybridize/bind complementary oligonucleotides.

## Materials and Methods

### Synthesis of oligomers

Fmoc protected monomers (mT) were obtained following a protocol reported in the literature[14] . Monomers were purified by liquid chromatography on silica gel, eluted with $CH_2Cl_2$:$CH_3OH$ 10:1 (v/v) with 0.1 % formic acid.

The oligomers were assembled on the PAL-PEG resin on a 10 µmol scale by consecutive cycles of deprotection, coupling and capping reactions. Deprotection and capping reactions were performed by standard protocols. Coupling of Fmoc-Ala-OH and Fmoc-Gly-OH was performed using 10 equivalents of amino acid dissolved in DMSO: DMF 25:75 (v/v) at 0.4 M concentration, activated with 8 equivalents of HATU (0.32M in DMF) and NMM 14 equivalents for 1 hours. Coupling of mT is performed as follows: 5 equivalents of mT are dissolved at 0.2 M concentration in DMSO:DMF 25:75 (v/v), activated with N,N'-diisopropylcarbodiimide (DIC) 5 equivalents in the presence of 8 equivalents of hydroxybenzotriazole (HOBt) 0.45M in DMF . Coupling time was set at two hours. Oligomers were obtained with yields around 75%, as calculated by Fmoc test performed after the last coupling.

Oligomers were analyzed by RP-HPLC on a Phenomenex Jupiter Proteo 4µ (150 x 4,60 mm ) and purified on a Jupiter 10µ Proteo 90A° (100x21,20mm) column using gradients of acetonitrile (0.1% TFA) in water (0.1% TFA). Oligomers were characterized by mass spectrometry on a Thermo Scientific LCQ Fleet ion trap instrument. Sequences, mass spectrometry data and purification gradients are reported for each sequence.

(Gly-mT)$_6$Gly: HPLC gradient: from 10 to 40 % of acetonitrile (0.1% TFA) in water (0.1% TFA). Calculated mass: 1839,66, experimental: 1840.63; 920.46.

(Gly-mT)$_{10}$Gly: HPLC gradient: from 10 to 30 % of acetonitrile (0.1% TFA) in water (0.1% TFA) ). Calculated mass: 3016,71, experimental: 1509.01, 1006.42 .

(Ala-mT)$_6$Ala: HPLC gradient: from 10 to 25 % of acetonitrile (0.1% TFA) in water (0.1% TFA). Calculated mass: 1937.82 experimental: 1937.61, 969.61.

**Molecular dynamic simulations**

Force field parameters for mT residue were generated by following a protocol reported previously for similar systems.[12,15] The starting geometries for mTGly$_6$/dA$_6$, 2mTGly$_6$/dA$_6$ and dT$_6$/A$_6$ were generated using the MOE software[16]. A double helix dT$_6$/A$_6$ hexamer was initially constructed using the RNA/DNA builder implemented in MOE. The geometry was minimized up to a gradient of 0.1 kcal/mol/Å using the default Amber10EHT force field coupled to the Born solvation model for water. This structure was also used as a template to build the mTGly$_6$/dA$_6$ hybrid by replacing each dT unit by mTGly. The resulting structure was minimized as described above. To build the 2mTGly$_6$/dA$_6$ hybrid, the mTGly$_6$/dA$_6$ model realized previously was overlaid to the NMR structure of a DNA triplex (chain A: 5'-d(GACTGAGAGACGTA)-3'; chain B: 5'-d(TACGTCTCTCAGTC)-3'; chain C: 5'-d(CTCTCT)-3') deposed in the Protein Data Bank as 1BWG.[17] Then, chain C was modified by replacing each C or T unit with mTGly and the triplex model was energy minimized as explained before.

Molecular dynamics (MD) simulations were conducted and analysed with the Amber18 and AmberTools19 packages,[18] using the ff14SB[19] and parmbsc1[20] forcefields for the peptide and DNA components, respectively, and the TIP3P model for water.[21] Parameters for the peptide bond rotation were modified as suggested by Doshi and Hemelberg[22]. Both classical and accelerated MD simulations were performed by following a protocol reported previously[22]. After a multistep equilibration phase, 20 ns of MD simulations were performed at constant number of particles, pressure and temperature (NPT) for mTGly$_6$/dA$_6$, dT$_6$/dA$_6$ and 2mTGly$_6$/dA$_6$ models. For this latter model, the last 10 ns of classical MD simulation results were also used to derive the boost parameters for the subsequent aMD run (average EPTOT = -31609.0 kcal/mol, average DHIED = 426.8 kcal/mol, total number of atoms = 10000, ethreshd = 545.8 kcal/mol, alphad = 23.8 kcal/mol, ethreshp = -30009.0 kcal/mol, alphap=1600.0 kcal/mol). Production aMD runs were conducted for 900 ns, under the NPT condition at 300 K, using a Langevin thermostat with a collision frequency of 2.0 ps$^{-1}$, a cut-off of 8.0 Å for electrostatics, the Particle mesh Ewald (PME) for long-range electrostatics[23], and the SHAKE algorithm to constrain bonds involving hydrogens[24]. All simulations were conducted using *pmemd.cuda* [25] and analysed with *cpptraj*[22]. Both classical and aMD trajectories were clustered into 10 clusters using the average-linkage algorithm and the pairwise mass-weighted root mean squared deviation (RMSD) on the Cα and P atoms. [22]

**Results and discussion**

**Oligomer synthesis**

 Oligomers containing 6 and 10 residues of the morpholino nucleosides, alternated with an amino acid (glycine or alanine) were obtained. The structure of the morpholino building block is reported in Figure 1; the sequences of the synthesized oligomers are reported in the Supplementary, Table 1. Oligomers were assembled by solid phase synthesis, using DIC/HOBt as activators to couple the mT monomers. Yields of the oligomers were in average 75%, as calculated by Fmoc test performed after the coupling of the last monomer Protocols to obtain the morpholino monomer (mT) and the oligomers are reported in the Supplementary Information.

**CD studies**

The secondary structure of the single stranded oligomers and also the ability of the oligomers to form complexes with DNA were investigated by Circular Dichroism.

The single stranded mTGly$_6$ CD spectrum shows an intense positive band around 220 nm, and two bands of about the same intensity centered at 250 and 275 nm (exciton band), that are respectively negative and positive (Figure 2). These signals are consistent with a certain degree of stacking between bases, that might suggest the existence of the oligomer in a B-like helix.

Formation of complexes with complementary DNA was investigated by CD. Complexes were obtained after an annealing process. We initially compared the spectra of the annealed mixtures with the spectra obtained by summing the CD spectra of all the single strands that were annealed. Superimposition of the spectra recorded for the 1:1 mixture of mTGly$_6$/dA$_6$ with that obtained by summing the contributes of single stranded dA$_6$ and mTGly$_6$ revealed no interaction between the strands. However, when mTGly$_6$ is annealed to dA$_6$ in a 2:1 molar ratio, the spectra of the mixture and the spectra deriving from the sum of all single strands were not superimposable, suggesting the formation of a complex (Figure 2B).

Polypyrimidine sequences may hybridize polypurine sequences by forming triple helices where nucleobases are kept together by H-bonds between bases (either Watson Crick and Hoogsteen) and by stacking interactions. The CD spectra of triple helices are in many cases similar to that of duplexes, but spectra deriving from the sum of single strands signals differ from the spectra of the hybrids in all their bands.

In the present case, instead, the band around 250 nm is superimposable in the spectra of the sample obtained after annealing of mTGly$_6$ and dA$_6$ and in the sum spectrum, suggesting the formation of a complex of a different nature. Thermal denaturation of this hybrid, followed by monitoring the increase in the intensity of the signal at 217 nm at increasing temperature, reveals a melting temperature of about 25°C (Figure 2C). When hybridization experiments are performed in a 2:1 stoichiometry using a DNA strand containing a mismatch (dA$_6$mis), we observe the formation of a complex again. Thermal denaturation occurs in this case at the same temperature observed for the fully matched complex, suggesting that the complex is not stabilized by specific H-bonds between the bases. These results indicate that the double or triple helices hybrids are not formed, likely as the distance between the nucleobases in the morpholino nucleopeptide does not match the distance between nucleobases in the DNA strand. On the other hand, the morpholino-amino acid single strand mTGly$_6$ binds to a single strand oligonucleotide. To further investigate on this issue, molecular dynamic (MD) simulations were performed, as explained later.

The oligomer mTGly$_{10}$ was also investigated. The CD of the single strand is very similar to that observed for the mTGly$_6$. Indeed, mTGly$_{10}$, unlike the shorter mTGly$_6$ does not form hybrids or complexes with dA$_{10}$ in a 1:1 and 2:1 molar ratio.

Next, we investigated the effect of the introduction of a further chiral center in the oligomer by replacing glycine with the helicogenic alanine. CD spectra recorded for the oligomer mTAla$_6$ show signals similar to those observed for mTGly$_6$, although less intense (Figure S1A). Unlike mTGly$_6$, the oligomer with alanine is not able to hybridize the complementary dA$_6$ in stoichiometry 1:1 and 2:1 (Figure S1B). Distances between nucleobases and steric hindrance of the methyl on the peptide side chain might contribute to prevent formation of mTAla$_6$ oligomer/dA$_6$ complexes.

**Molecular modelling**

We initially compared the structure of a $dT_6$ single strand with that of $mTGly_6$ to see if, at least theoretically, the nucleobases could maintain the same distances in the two polymers. Indeed, the N1-thymine nitrogens are separated by ten atoms in both structures. We thus aligned the $dT_6$ and $mTGly_6$ strands using the flexible alignment tool of the MOE software. The obtained superposition is shown in Supplementary Figure S1. As expected, the nucleobases of $dT_6$ and $mTGly_6$ are well superimposed, but a severe mismatch can be observed for the backbone, possibly due to the different number of atoms found between two consecutive 5' oxygens of $dT_6$ or between two glycine NH groups in $mTGly_6$ (five and six, respectively).

To evaluate how this backbone mismatch can influence the formation of DNA/$mTGly_6$ hybrids, the conformational behaviour of $mTGly_6/dA_6$ and $2mTGly_6/dA_6$ hybrids was analysed by MD simulations. The starting structure of $mTGly_6/dA_6$ (Figure 3A) was prepared based on an ideal $dT_6/dA_6$ duplex by replacing each T nucleotide by a mTGly monomer. Conversely, the $mTGly_6/mTGly_6/dA_6$ hybrid (Figure 3C) was constructed using the NMR structure of a DNA triplex, available in the Protein Data Bank (PDB code 1BWG),[17] as a template. Both systems were then subjected to 20 ns of MD simulation. A model of $dT_6/dA_6$ was also subjected to the same protocol and used as a reference.

The cluster analysis of the MD trajectories showed that most of the Watson Crick interactions between the $mTGly_6$ and $dA_6$ chains were lost in both duplex and triplex models (Figures3 B,D, respectively), while the reference $dT_6/dA_6$ remained stable (Supplementary Figure S2).

These behaviours were also confirmed by the time-dependent analysis of the root mean square displacement (RMSD). Both $mTGly_6/dA_6$ and $2mTGly_6/dA_6$ hybrids resulted indeed highly unstable, contrarily to what has been observed for the $dT_6/dA_6$ reference (Supplementary Figure S3). Based on CD experiments, instability was expected for the $mTGly_6/dA_6$ hybrid but some interactions were expected for $2mTGly_6/dA_6$. However, we noticed that the two $mTGly_6$ strands quickly rearranged to a β-sheet like structure during the 20 ns of MD (Figure 3 D). This led to the hypothesis that, when a 2:1 molar ratio is used, aggregates could be formed through a $(mTGly_6)_2$ β-sheet-like structure that eventually captures the $dA_6$ single strand.

Aggregation is a process that might be too long for being described by classical MD simulations, but it can be accessible by enhanced sampling (ES) methods.[26],[27] Moreover, we recently used ES calculations to define the conformational preferences of non-natural peptides based on morpholino amino acids.[12], [15] Among ES methods, accelerated MD (aMD) can sample events occurring at the millisecond timescale but with simulations of a few hundreds of nanoseconds only, and at a reasonable computational cost.[28] Thus, starting from the last frame of the 20 ns classical MD trajectory described previously, we subjected the $2mTGly_6/dA_6$ hybrid to 900 ns of aMD simulation[29].

As expected, the analysis of the obtained trajectory did not show any Watson Crick nor Hoogsteen base pairing. However, the formation of an aggregate showing backbone-backbone, backbone-base and base-base H-bonds (Supplementary Table 2) was instead observed. Interestingly, among the more stable H-bonds between two $mTGly_6$ strands, we found two typical of the anti-parallel β-

sheet: one is between the C=O$_{Gly2}$ of chain 1 and the NH$_{Gly5}$ of chain 2 (Occ% = 41.7), the other is between the C=O$_{Gly3}$ of chain 1 and the NH$_{Gly3}$ of chain 2 (Occ% = 39.4).


The dA$_6$ DNA strand seems to interact with the 2mTGly$_6$ dimer stably, but aspecifically. Indeed, when looking at the structure of the representative geometry of the two most populated conformational clusters (Figure 4), we observe no base pairing and no preferred conformation for the dA$_6$ chain. When the most populated cluster is considered (Figure 4 A), we can see several but labile (Occ% < 20) H-bonds involving either the bases or the phosphate backbone. According to Table 2, the only relevant H-bond involving dA$_6$ is found between the NH$_2$ group of dA2 and the C=O$_{T5}$ of mTGly$_6$ chain 2 (Occ% = 28.3). Indeed, this H-bond is also observed in the representative structure of the second most populated cluster (Figure 4 B).
In conclusion, theoretical calculations show that interactions are not favoured between a single mTGly$_6$ strand and dA$_6$. However, in a 2:1 molar ratio, mTGly$_6$ can bind dA$_6$ to give a complex that is not stabilized by   Watson Crick or Hoogsteen hydrogen bonds. Indeed, we see that the two mTGly$_6$ chains have some tendency to form antiparallel β-sheet-like aggregates, while the interaction with dA$_6$ is mostly driven by an H-bond with dA2 and by hydrophobic contacts between the nucleobases.

In conclusion, oligomers composed of alternating amino acids and morpholino-like nucleic acids were obtained. Single stranded oligomers show some degree of secondary structure characterized by nucleobases stacking, as suggested by CD, but none of the synthesized compound is able to form canonical H-bonds with complementary DNA. Indeed, mTGly$_6$ oligomer containing glycine is more flexible and forms complexes with dA$_6$ in a 2:1 molar ratio. Investigation carried out by MD simulations suggests the formation of aggregates stabilised by H-bonds between two peptide backbones, forming an antiparallel sheet, and hydrophobic interaction between this construct and the nucleobase strand.
As far as we introduce a chiral center in the backbone (as in mTAla$_6$) or we increase the oligomer length (as in mTGly$_{10}$), the flexibility of the oligomer decreases, preventing formation of complexes.
The ability of mTGly$_6$ to form complexes with oligonucleotides opens the way to their application in the delivery of nucleic acids.

## References

[1] C. Avitabile, A. Cimmino, A. Romanelli, Oligonucleotide analogues as modulators of the expression and function of noncoding RNAs (ncRNAs): Emerging therapeutics applications, J. Med. Chem. 57 (2014). https://doi.org/10.1021/jm5006594.

[2] E. Subbotina, S. Koganti, D. Hodgson-Zingman, L. Zingman, Morpholino-driven gene editing: A new horizon for disease treatment and prevention, Clin. Pharmacol. Ther. (2016). https://doi.org/10.1002/cpt.276.

[3] S. Pensato, M. Saviano, A. Romanelli, New peptide nucleic acid analogues: Synthesis and applications, Expert Opin. Biol. Ther. 7 (2007). https://doi.org/10.1517/14712598.7.8.1219.

[4] C.I. Edvard Smith, R. Zain, Therapeutic oligonucleotides: State of the art, Annu. Rev. Pharmacol. Toxicol. (2019). https://doi.org/10.1146/annurev-pharmtox-010818-021050.

[5] P. Wang, T.A. Meyer, V. Pan, P.K. Dutta, Y. Ke, The Beauty and Utility of DNA Origami, Chem. (2017). https://doi.org/10.1016/j.chempr.2017.02.009.

[6] D. Mathur, I.L. Medintz, The Growing Development of DNA Nanostructures for Potential Healthcare-Related Applications, Adv. Healthc. Mater. (2019). https://doi.org/10.1002/adhm.201801546.

[7] C. Avitabile, C. Diaferia, B. Della Ventura, F.A. Mercurio, M. Leone, V. Roviello, M. Saviano, R. Velotta, G. Morelli, A. Accardo, A. Romanelli, Self-Assembling of Fmoc-GC Peptide Nucleic Acid Dimers into Highly Fluorescent Aggregates, Chem. - A Eur. J. (2018). https://doi.org/10.1002/chem.201800279.

[8] C. Avitabile, C. Diaferia, V. Roviello, D. Altamura, C. Giannini, L. Vitagliano, A. Accardo, A. Romanelli, Fluorescence and Morphology of Self-Assembled Nucleobases and Their Diphenylalanine Hybrid Aggregates, Chem. - A Eur. J. (2019). https://doi.org/10.1002/chem.201902709.

[9] G.N. Roviello, D. Musumeci, E.M. Bucci, C. Pedone, Evidences for supramolecular organization of nucleopeptides: Synthesis, spectroscopic and biological studies of a novel dithymine l-serine tetrapeptide, Mol. Biosyst. (2011). https://doi.org/10.1039/c0mb00214c.

[10] G.N. Roviello, C. Vicidomini, S. Di Gaetano, D. Capasso, D. Musumeci, V. Roviello, Solid phase synthesis and RNA-binding activity of an arginine-containing nucleopeptide, RSC Adv. (2016). https://doi.org/10.1039/c5ra25809j.

[11] X. Li, Y. Kuang, H.C. Lin, Y. Gao, J. Shi, B. Xu, Supramolecular nanofibers and hydrogels of nucleopeptides, Angew. Chemie - Int. Ed. (2011). https://doi.org/10.1002/anie.201103641.

[12] F. Vaghi, R. Bucci, F. Clerici, A. Contini, M.L. Gelmi, Non-natural 3-Arylmorpholino-β-amino Acid as a PPII Helix Inducer, Org. Lett. (2020). https://doi.org/10.1021/acs.orglett.0c02331.

[13] C.A. Rohl, W. Fiori, R.L. Baldwin, Alanine is helix-stabilizing in both template-nucleated and standard peptide helices, Proc. Natl. Acad. Sci. U. S. A. (1999). https://doi.org/10.1073/pnas.96.7.3682.

[14] R. Bucci, A. Bossi, E. Erba, F. Vaghi, A. Saha, S. Yuran, D. Maggioni, M.L. Gelmi, M. Reches, S. Pellegrino, Nucleobase morpholino β amino acids as molecular chimeras for the preparation

of photoluminescent materials from ribonucleosides, Sci. Rep. (2020). https://doi.org/10.1038/s41598-020-76297-7.

[15] R. Bucci, A. Contini, F. Clerici, S. Pellegrino, M.L. Gelmi, From glucose to enantiopure morpholino β-amino acid: A new tool for stabilizing γ-turns in peptides, Org. Chem. Front. (2019). https://doi.org/10.1039/c8qo01116h.

[16] C.C.G. ULC, Molecular Operating Environment (MOE), 2013.08, 1010 Sherbooke St. West, Suite #910, Montr. QC, Canada, H3A 2R7. (2018).

[17] J.L. Asensio, T. Brown, A.N. Lane, Solution conformation of a parallel DNA triple helix with 5' and 3' triplex-duplex junctions, Structure. (1999). https://doi.org/10.1016/S0969-2126(99)80004-5.

[18] D.A. Case, I.Y. Ben-Shalom, S.R. Brozell, D.S. Cerutti, T.E. Cheatham, V.W.D.C. III, T.A. Darden, R.E. Duke, D. Ghoreishi, M.K. Gilson, H. Gohlke, A.W. Goetz, D. Greene, R Harris, N. Homeyer, S. Izadi, A. Kovalenko, T. Kurtzman, T.S. Lee, S. LeGrand, P. Li, C. Lin, J. Liu, T. Luchko, R. Luo, D.J. Mermelstein, K.M. Merz, Y. Miao, G. Monard, C. Nguyen, H. Nguyen, I. Omelyan, A. Onufriev, F. Pan, R. Qi, D.R. Roe, A. Roitberg, C. Sagui, S. Schott-Verdugo, J. Shen, C.L. Simmerling, J. Smith, R. Salomon-Ferrer, J. Swails, R.C. Walker, J. Wang, H. Wei, R.M. Wolf, X. Wu, L. Xiao, D.M. York, P.A. Kollman, AMBER 2018, University of California, 2018.

[19] J.A. Maier, C. Martinez, K. Kasavajhala, L. Wickstrom, K.E. Hauser, C. Simmerling, ff14SB: Improving the Accuracy of Protein Side Chain and Backbone Parameters from ff99SB, J. Chem. Theory Comput. (2015). https://doi.org/10.1021/acs.jctc.5b00255.

[20] I. Ivani, P.D. Dans, A. Noy, A. Pérez, I. Faustino, A. Hospital, J. Walther, P. Andrio, R. Goñi, A. Balaceanu, G. Portella, F. Battistini, J.L. Gelpí, C. González, M. Vendruscolo, C.A. Laughton, S.A. Harris, D.A. Case, M. Orozco, Parmbsc1: A refined force field for DNA simulations, Nat. Methods. (2015). https://doi.org/10.1038/nmeth.3658.

[21] W.L. Jorgensen, J. Chandrasekhar, J.D. Madura, R.W. Impey, M.L. Klein, Comparison of simple potential functions for simulating liquid water, J. Chem. Phys. (1983). https://doi.org/10.1063/1.445869.

[22] U. Doshi, D. Hamelberg, Reoptimization of the AMBER force field parameters for peptide bond (Omega) torsions using accelerated molecular dynamics, J. Phys. Chem. B. (2009). https://doi.org/10.1021/jp907388m.

[23] T. Darden, D. York, L. Pedersen, Particle mesh Ewald: An N·log(N) method for Ewald sums in large systems, J. Chem. Phys. (1993). https://doi.org/10.1063/1.464397.

[24] J.P. Ryckaert, G. Ciccotti, H.J.C. Berendsen, Numerical integration of the cartesian equations of motion of a system with constraints: molecular dynamics of n-alkanes, J. Comput. Phys. (1977). https://doi.org/10.1016/0021-9991(77)90098-5.

[25] R. Salomon-Ferrer, A.W. Götz, D. Poole, S. Le Grand, R.C. Walker, Routine microsecond molecular dynamics simulations with AMBER on GPUs. 2. Explicit solvent particle mesh ewald, J. Chem. Theory Comput. (2013). https://doi.org/10.1021/ct400314y.

[26] Y. Jin, Y. Sun, Y. Chen, J. Lei, G. Wei, Molecular dynamics simulations reveal the mechanism

of graphene oxide nanosheet inhibition of Aβ1-42 peptide aggregation, Phys. Chem. Chem. Phys. (2019). https://doi.org/10.1039/c9cp01803d.

[27]  A. Morriss-Andrews, J.E. Shea, Computational studies of protein aggregation: Methods and applications, Annu. Rev. Phys. Chem. (2015). https://doi.org/10.1146/annurev-physchem-040513-103738.

[28]  L.C.T. Pierce, R. Salomon-Ferrer, C. Augusto F. De Oliveira, J.A. McCammon, R.C. Walker, Routine access to millisecond time scale events with accelerated molecular dynamics, J. Chem. Theory Comput. (2012). https://doi.org/10.1021/ct300284c.

[29]  D. Hamelberg, J. Mongan, J.A. McCammon, Accelerated molecular dynamics: A promising and efficient simulation method for biomolecules, J. Chem. Phys. (2004). https://doi.org/10.1063/1.1755656.

**Legend to figures**

**Figure 1**: A) Building blocks employed in the synthesis of the oligomers; on the left side the "morpholino-T" (mT), on the right the amino acids. B) Chemical structure of the oligomers obtained (n= 6 or 10).

**Figure 2**: A) CD spectrum of mTGly$_6$ oligomer at 6µM; B) superimposition of the CD spectra of the annealed mTGly$_6$/dA$_6$ mixture in a 2:1 molar ratio (concentration of dA$_6$= 3µM) at 10°C (blue) with the sum spectrum, obtained summing CD spectra of mTGly$_6$ (6µM)+dA$_6$(3µM) (black); C) melting profile followed at 217 nm for the annealed mTGly$_6$/dA$_6$ mixture in a 2:1 molar ratio (concentration of dA$_6$= 3µM). Experiments were carried in sodium phosphate buffer 10 mM, pH 7.0.

**Figure 3**. Starting geometries (A, C) and representative structures of the most populated cluster (B, cluster population = 38.6% and D, cluster population = 69.6%) obtained by cluster analysis of the last 10 ns of a 20 ns MD trajectory of the mTGly$_6$/dA$_6$ and 2mTGly$_6$/dA$_6$ hybrids, respectively. dA$_6$ chains are always represented with carbon atoms coloured in orange. The mTGly$_6$ chains are depicted with carbon atoms coloured in green (mTGly$_6$/dA$_6$ hybrid) or green and turquoise (2mTGly$_6$/dA$_6$ hybrid).

**Figure 4**. Representative geometries of the first (panel A; cluster population = 33.5%) and second (panel B; population = 27.2%) most populated clusters obtained by cluster analysis of the 900 ns aMD trajectory of the 2mTGly$_6$/dA$_6$ hybrid (carbon atoms are coloured in green and turquoise for mTGly$_6$ chains 1 and 2, respectively, in orange for dA$_6$).
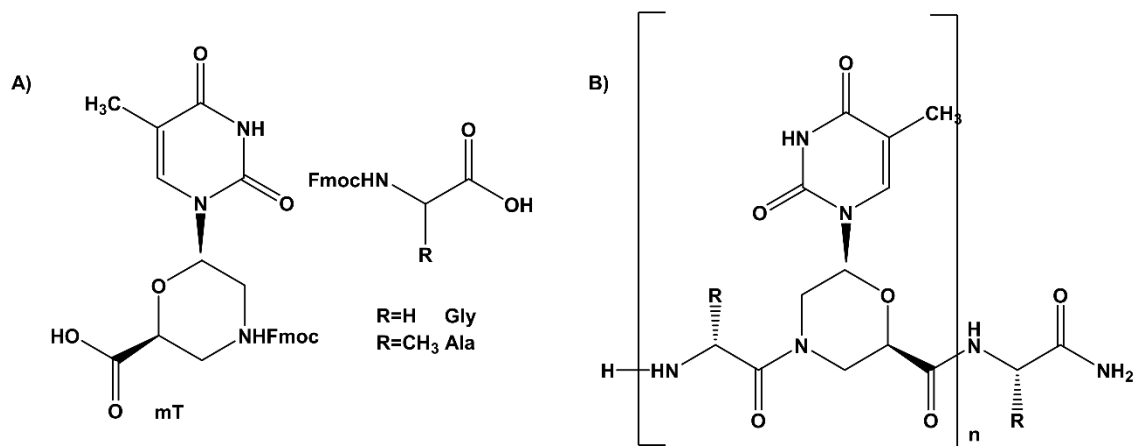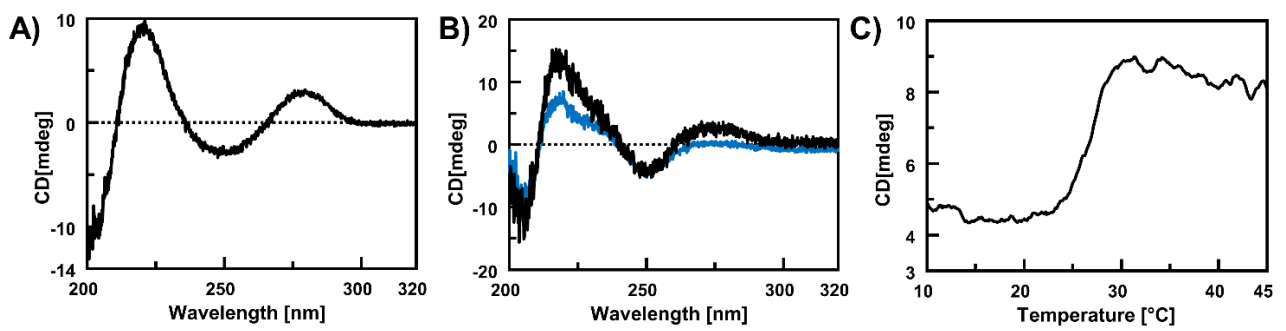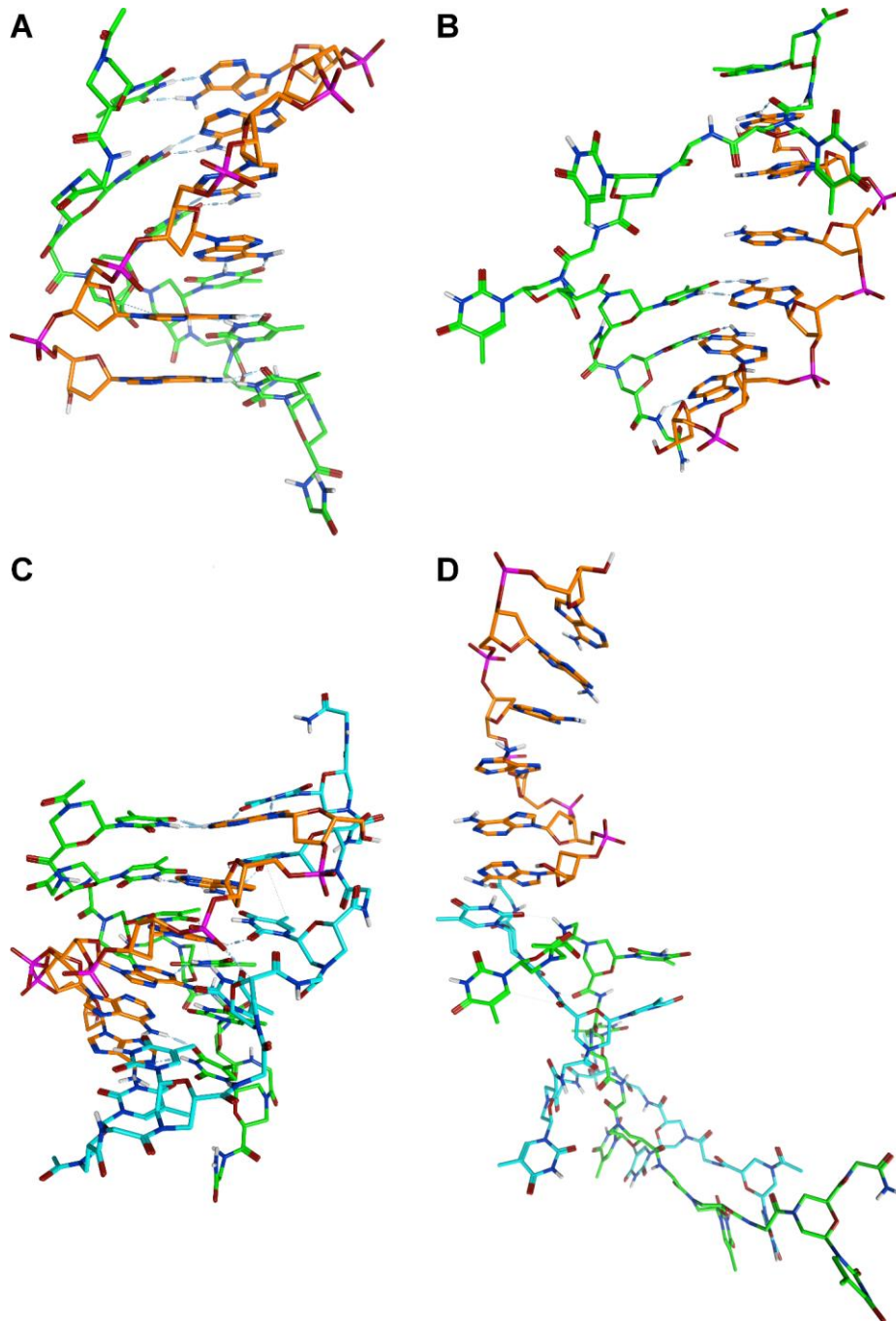
## FIGURE 1



## FIGURE 2

FIGURE 3

FIGURE 4



A

B